Popular Summary of

The Arctic Vortex in March 2011: A Dynamical Perspective

Submitted to Atmospheric Chemistry and Physics, July 2011

Margaret M. Hurwitz [1,2], **Paul A. Newman** [2], and **Chaim I. Garfinkel** [3]

1 *Goddard Earth Sciences Technology and Research (GESTAR), Morgan State Popular Summary of*

The Arctic Vortex in March 2011: A Dynamical Perspective

Submitted to Atmospheric Chemistry and Physics, July 2011

Margaret M. Hurwitz [1,2], **Paul A. Newman** [2], and **Chaim I. Garfinkel** [3]

1 *Goddard Earth Sciences Technology and Research (GESTAR), Morgan State University, Baltimore, MD, USA*

2 *NASA Goddard Space Flight Center, Greenbelt, MD, USA*

3 *Johns Hopkins University, Baltimore, MD, USA*

In late winter in the Arctic stratosphere, ozone loss is closely tied to temperature: Ozone–depleting substances (e.g., CFCs) are activated on polar stratospheric clouds, which form only at very low temperatures. Variability in polar lower stratospheric temperature is highly correlated with the year–to–year variability in large–scale wave driving from the troposphere.

Record ozone loss was observed in March 2011. This paper documents the dynamical conditions associated with this event: Weak wave driving in February preceded cold anomalies in the polar lower stratosphere in March and a relatively late winter–to–spring transition in April. The 2011 conditions were unusual with respect to the 1979–2011 satellite era, but not unprecedented. Similarly severe ozone loss, low temperatures and weak wave driving were observed in March 1997.

In March 2011, El Niño/Southern Oscillation was in its cold phase (i.e., La Niña) while the quasi-biennial oscillation (QBO), an alternating east-west wind pattern in the equatorial lower stratosphere, was in its westerly phase. Though both of these conditions are generally associated with a colder lower stratosphere in mid-winter, the respective cold anomalies do not persist through March. Therefore, the La Niña and QBO-westerly conditions cannot explain the observed cold anomalies in March 2011. In contrast, positive sea surface temperature anomalies in the North Pacific may have contributed to the unusually weak tropospheric wave driving and cold Arctic stratosphere in late winter 1997 and 2011.

University, Baltimore, MD, USA

2 *NASA Goddard Space Flight Center, Greenbelt, MD, USA*

3 *Johns Hopkins University, Baltimore, MD, USA*

In late winter in the Arctic stratosphere, ozone loss is closely tied to temperature: Ozone-depleting substances (e.g., CFCs) are activated on polar stratospheric clouds, which form only at very low temperatures. Variability in polar lower stratospheric temperature is highly correlated with the year-to-year variability in large-scale wave driving from the troposphere.

Record ozone loss was observed in March 2011. This paper documents the dynamical conditions associated with this event: Weak wave driving in February preceded cold anomalies in the polar lower stratosphere in March and a relatively late winter-to-spring transition in April. The 2011 conditions were unusual with respect to the 1979–2011 satellite era, but not unprecedented. Similarly severe ozone loss, low temperatures and weak wave driving were observed in March 1997.

In March 2011, El Niño/Southern Oscillation was in its cold phase (i.e., La Niña) while the quasi-biennial oscillation (QBO), an alternating east-west wind pattern in the equatorial lower stratosphere, was in its westerly phase. Though both of these conditions are generally associated with a colder lower stratosphere in mid-winter, the respective cold anomalies do not persist through March. Therefore, the La Niña and QBO-westerly conditions cannot explain the observed cold anomalies in March 2011. In contrast, positive sea surface temperature anomalies in the North Pacific may have contributed to the unusually weak tropospheric wave driving and cold Arctic stratosphere in late winter 1997 and 2011.

The Arctic Vortex in March 2011: A Dynamical Perspective

Margaret M. Hurwitz [1, 2], **Paul A. Newman** [2] and **Chaim I. Garfinkel** [3]

[1] {Goddard Earth Sciences Technology and Research (GESTAR), Morgan State University, Baltimore, MD, USA}

[2] {NASA Goddard Space Flight Center, Greenbelt, MD, USA}

[3] {Johns Hopkins University, Baltimore, MD, USA}

Correspondence to: Margaret M. Hurwitz (margaret.m.hurwitz@nasa.gov)

Abstract

Despite the record ozone loss observed in March 2011, dynamical conditions in the Arctic stratosphere were unusual but not unprecedented. Weak planetary wave driving in February preceded cold anomalies in the polar lower stratosphere in March and a relatively late breakup of the Arctic vortex in April. La Niña conditions and the westerly phase of the quasi–biennial oscillation (QBO) were observed in March 2011. Though these conditions are generally associated with a stronger vortex in mid–winter, the respective cold anomalies do not persist through March. Therefore, the La Niña and QBO–westerly conditions cannot explain the observed cold anomalies in March 2011. In contrast, positive sea surface temperature anomalies in the North Pacific may have contributed to the unusually weak tropospheric wave driving and strong Arctic vortex in late winter 2011.

1 Introduction

In the Arctic stratosphere, chemical ozone loss takes place each year in the late winter (WMO, 2011). Arctic ozone loss represents the interaction between chemistry and climate: heterogeneous ozone depletion on polar stratospheric clouds requires the presence of halogens, sunlight and low temperatures. Rex et al. (2004 and 2006) calculated that the severity of large ozone loss events has been increasing over the last few decades, and speculated that increased radiative cooling by greenhouse gases plays a role.

Severe ozone loss was observed in the Arctic stratosphere in 2011. On March 14th, the Alfred Wegener Institute (AWI) in Germany reported that "unusually low temperatures in the Arctic ozone layer have recently initiated massive ozone depletion" (http://www.awi.de/en/news/press_releases). Figure 1a shows that March 2011 monthly mean total ozone value was the lowest of the satellite era (total ozone dataset updated from Stolarski and Frith, 2006). On April 8th, Science Daily reported "unprecedented" Arctic ozone depletion, caused by unusual and persistent cold conditions in the Arctic vortex (http://www.sciencedaily.com/releases/2011/04/110406085634.htm). Researchers at AWI noted that the anomalous ozone loss and low temperatures in March 2011 were consistent with the estimated pattern of "cold winters getting colder" (Rex et al., 2004 and 2006).

Two sources of interannual variability in the Arctic lower stratosphere in winter are El Niño/Southern Oscillation (ENSO) and the phase of the quasi–biennial oscillation (QBO). Holton and Tan (1980) and Lu et al. (2008) showed that the phase of the QBO modulates the region in which planetary waves can propagate in the stratosphere, thus affecting the strength of the Arctic vortex in mid–winter. The vortex is strongest during the westerly phase of the QBO. Similarly, planetary wave driving is stronger during El Niño (ENSO warm phase) events than during La Niña (ENSO cold phase) events (e.g., Garfinkel and Hartmann, 2008).

The goals of this paper are to document the dynamical conditions in the Arctic stratosphere in March 2011 and attribute these conditions to known sources of dynamical variability. Section 2 will describe the datasets and diagnostics used to perform this analysis. In Section 3, March 2011 will be examined in the context of the satellite era. The relationship of March conditions in the Arctic stratosphere to ENSO and the phase of the QBO will be considered. In addition, the possible role of North Pacific sea surface temperature variability in the anomalous dynamical conditions in the Arctic vortex in March 2011 will be examined. Section 4 will provide a brief summary and discussion.

2 Data and diagnostics

Sea surface temperature (SST) and atmospheric diagnostics are used to understand conditions in the Arctic stratosphere in March 2011. The present analysis spans the satellite era (1979–2011) and focuses on the Northern Hemisphere mid– to late winter (January through March). Zonal winds, temperature and eddy heat flux fields are derived from the National Centers for Environmental Prediction (NCEP)–U.S. Department of Energy (DOE) reanalysis (NCEP–2) (Kanamitsu et al., 2002). The NCEP–2 reanalysis has 2.5° x 2.5° horizontal resolution and vertical coverage up to 10 hPa.

The phase of the quasi–biennial oscillation (QBO) is characterized by zonal winds in the equatorial region at 50 hPa. Monthly mean values of the 50–hPa QBO index (http://www.cpc.ncep.noaa.gov/data/indices/qbo.u50.index) are used in this study.

The springtime breakup of the Arctic vortex is calculated for each year. On the 450 K isentropic surface (i.e., in the lower stratosphere), the breakup date is defined as the date when the five–day running mean of zonal winds at the vortex edge falls below approximately 15.2 m s^{-1}, following the criteria of Nash et al. (1996). The present analysis considers breakup dates based on the NCEP–1 (Kalnay et al., 1996), NCEP–2 and NOAA Climate Prediction Center (CPC) (Gelman et al., 1986; Nagatani et al., 1988; Finger et al., 1993) meteorological reanalyses.

Monthly mean SST fields are taken from the Hadley Centre Global Sea Ice and Sea Surface Temperature (HadISST1) dataset (Rayner et al., 2003). Sea surface temperature anomalies in the eastern equatorial Pacific are characterized by the Niño 3.4 index (see http://www.cpc.noaa.gov/data/indices). Trenberth (1997) defines a conventional El Niño event as a sustained period (usually six months or more) when the Niño 3.4 index exceeds 0.4, while a La Niña event is defined as a sustained period when the Niño 3.4 index is less than –0.4.

3 Results

3.1 March 2011 in a historical context

In March 2011, the Arctic vortex was colder, stronger and more persistent than usual. Figure 1 shows histograms of the polar cap temperature, breakup date of the Arctic vortex, ENSO index, QBO index and North Pacific SST index in the Arctic late winter 2011 with respect to the 1979–2011 period. A histogram of March mean temperatures for the Arctic polar cap at 50 hPa is shown in Figure 1b. The March 2011 temperature of 208.5 K (indicated by the red outline) is more than two standard deviations lower than the climatological mean value (216.8 K) and is the second–lowest value in the 1979–2011 period. The lowest value (206.1 K, indicated by the blue outline) occurred in 1997.

The breakup of the Arctic vortex occurs in late winter. A histogram of breakup dates at 450 K is shown in Figure 1c. The breakup date in 2011 was 19th April in the NCEP–2 reanalysis, later than the mean date of 20th March in the NCEP reanalyses and 10th April in the CPC reanalysis. The breakup date in 2011 was, depending on the zonal wind dataset, either the third or fourth latest of the satellite era. The late breakup of the Arctic vortex is consistent with the low temperatures and total ozone observed in March 2011 (see Figures 1a and 1b).

Unusually cold conditions in the Arctic stratosphere in March 2011 correspond with unusually weak planetary wave driving in February 2011. Newman et al. (2001) found that polar lower stratospheric temperature is correlated with mid–latitude eddy heat flux at 100 hPa, with a 1–2 month lag; this finding suggests that weaker than usual eddy heat flux in February should correspond with a colder than usual Arctic lower stratosphere in March. Figure 2 shows that February eddy heat flux and March polar cap temperature at 50 hPa are indeed well correlated, and highlights the unusually low values observed in 2011.

March temperature anomalies in 2011 and 1997 are shown in Figures 3a and 3b. In both 1997 and 2011, the Arctic stratosphere cooled strongly while the mid–latitudes and Arctic troposphere warmed weakly. Consistent with the temperature differences, zonal winds were relatively stronger at high latitudes; peak wind differences exceeded 20 m s^{-1} at 10 hPa at high latitudes (not shown). The magnitude of the stratospheric cooling was larger in 1997 than in 2011. February eddy heat flux was weaker in 1997 than in 2011 as well (see Figure 2).

3.2 Influence of ENSO and the QBO on the Arctic stratosphere in March

La Niña and QBO–westerly conditions persisted through March 2011. The Niño 3.4 index was strongly negative in January through March 2011, indicating La Niña conditions (Figure 1d). In March 2011, equatorial zonal winds at 50 hPa were approximately 6 m s^{-1} (Figure 1e), indicating the westerly phase of the QBO.

This section compares the temperature anomalies observed in March 2011 with those observed during typical La Niña conditions and during the westerly phase of the QBO. The March temperature response to La Niña events is estimated by comparing years when the Niño 3.4 index is equal to or less than –1 (as in 2011) with years when the Niño 3.4 index is between –0.5 and 0.5 (i.e., ENSO neutral). Figure 3c shows that, in the Arctic stratosphere, the typical March temperature response to a La Niña event is a weak warming. The La Niña response is inconsistent with the observed temperature response in both 1997 and 2011.

The QBO was in its westerly phase during the 2010–2011 winter season (Figure 1e). The March temperature response to the phase of the QBO is estimated by comparing composites of QBO–westerly years and QBO–easterly years. The typical March temperature response is a relative warming of the Arctic stratosphere that increases with altitude (Figure 3d). As for the La Niña response, the temperature response to QBO–westerly conditions is inconsistent with the observed temperature response in both 1997 and 2011.

In summary, the patterns and magnitudes of the March 2011 temperatures differences from climatology are similar to those seen in March 1997, but different from the Arctic response to both La Niña events and to the phase of the QBO. March zonal wind and February eddy heat flux differences are consistent with these conclusions. That is, the weak eddy heat flux in February and low temperatures in March 2011 are not related to either ENSO or the QBO.

3.3 Influence of North Pacific SSTs on the Arctic stratosphere in March

This section considers the influence of extra–tropical SSTs on the Arctic stratosphere in March. March lower stratospheric temperature and February planetary wave driving should be most influenced by SST variability in the mid– to late winter. As noted in Section 3.2, January/February SSTs in the tropical Pacific and March polar cap temperatures are not correlated. However, SSTs in the North Pacific, poleward of 40°N and close to the dateline, are strongly negatively correlated with March polar cap temperatures. This region corresponds with the dominant mode of SST variability in the North Pacific in boreal winter i.e., the 'subarctic mode' identified by Nakamura et al., (1997). The subarctic mode is associated with SST variability at decadal timescales, caused by variability in the Kuroshio and Oyashio currents, and is not influenced by variability in the tropical Pacific (i.e., variability related to ENSO). Furthermore, the subarctic SST mode is not related to the Pacific Decadal Oscillation (PDO) (index updated from Mantua et al., 1997; Zhang et al., 1997).

The positive phase of the subarctic SST mode tends to weaken the Aleutian low and thus the Pacific–North American (PNA) circulation pattern. Garfinkel et al. (2010) found that variability of the Aleutian low modulates the strength of the Arctic vortex in mid–winter, with a similar relationship in late winter (not shown).

In this study, the subarctic SST index is defined as the January/February mean SST anomaly from the 1979–2011 climatology, in the 40–50°N, 160–200°E region. The subarctic SST index was strongly positive in both 1997 and 2011 (Figure 1f). Figure 3e shows the difference between March temperatures in years when the subarctic SST index is strongly positive as compared with years when the index is strongly negative: The Arctic stratosphere is relatively colder (by approximately 6 K at 50 hPa), while below 500 hPa the Arctic is approximately 2 K warmer. The structure and magnitude of these temperature differences are broadly consistent with the March temperature anomalies observed in 1997 and 2011 (Figures 3a and 3b), suggesting that North Pacific SST variability strongly contributed to variability in the Arctic stratosphere in March 1997 and 2011.

4 Discussion

Unusual dynamical conditions were observed in the Arctic stratosphere in March 2011. Tropospheric planetary wave driving was unusually weak, consistent with a strong, stable Arctic vortex in late winter and a relatively late vortex breakup. From a zonal mean perspective, the dynamical conditions observed in 2011 were not unprecedented: February eddy heat flux was weaker and March polar cap temperature was lower in 1997 than in 2011.

Recent cooling of the Arctic lower stratosphere has been reported by e.g., Randel et al. (2009) and Kennedy et al. (2010). In the NCEP–2 reanalysis in March, polar cap temperature at 50 hPa decreased 1.6 ± 1.3 K $year^{-1}$ during the 1979–2011 period. During this period, cooling of the Arctic lower stratosphere can be largely attributed to increased radiative forcing by greenhouse gases and to ozone depletion (Shine et al., 2003; Stolarski et al., 2010). However, this modest linear trend in March does not explain the anomalous conditions in 1997 and 2011, when the Arctic lower stratosphere was more than 10 K below the climatological mean.

Similarly, the phase of the 11–year solar cycle does not account for the anomalous conditions in March 2011. The solar cycle can be characterized by the solar flux at 2800 MHz (ftp://ftp.ngdc.noaa.gov/STP/SOLAR_DATA/SOLAR_RADIO/FLUX/Penticton_Observed/monthly/MONTHLY.OBS); both 1997 and 2011 were within a few years of solar minima. Since the QBO was easterly in 1997 but westerly in 2011, the product of the solar cycle and QBO anomalies had the opposite sign in 1997 as compared with 2011. Though this quantity is well correlated with polar variability (Haigh and Roscoe, 2006), it does not explain the anomalously strong vortex events in both 1997 and 2011.

ENSO and the QBO do not explain the unusual dynamical conditions in March 2011. While La Niña conditions tend to strengthen the Arctic vortex in mid–winter, the La Niña signal weakens and begins to reverse by March. In Goddard Earth Observing System Chemistry–Climate Model, Version 2 (GEOS V2 CCM) simulations (model formulation as described by Hurwitz et al., 2011), the Arctic lower stratosphere is cooler in March under La Niña and QBO–westerly conditions, as compared with ENSO neutral and QBO–easterly; however; the magnitude of this cooling is an order of magnitude less than observed in March 2011. Furthermore, the structure and magnitude of dynamical anomalies in the Arctic stratosphere were similar in March 1997 and March 2011, despite different phases of the QBO.

Positive SST anomalies in the North Pacific may have contributed to the anomalous conditions in March 2011. Positive SST anomalies in the 40–50°N, 160–200°E region in January and February, such as those observed in 1997 and 2011, are strongly anti–correlated with polar lower stratospheric temperature anomalies in March. Positive SSTs in this region tend to weaken the Aleutian low, leading to a reduced eddy heat flux entering the stratosphere (Garfinkel et al., 2010). The subarctic SST index in January/February and March polar cap temperature at 50 hPa are correlated at the 95% confidence level. However, the relationship between North Pacific SSTs and stratospheric variability is non–linear: While multiple linear regressions to either February eddy heat flux or March polar cap temperature show that the subarctic SST mode is, statistically, the dominant cause of dynamical variability, these linear regressions do not capture the extreme values seen in e.g., 1997 and 2011. A planned modelling study will, by comparing time–slice simulations of the positive and negative extremes of the subarctic SST mode, isolate the impact of North Pacific SSTs on Arctic dynamics and ozone in March.

Acknowledgements

The authors thank Eric Nash for providing vortex breakup dates, the chemistry–climate modelling group at NASA GSFC for helpful feedback and NASA's ACMAP program for funding.

References

Finger, F. G., Gelman, M. E., Wild, J. D., Chanin, M. L., Hauchecorne, A., and Miller, A. J.: Evaluation of NMC upper stratospheric temperature analyses using rocketsonde and lidar data, Bull. Am. Meteorol. Soc., 74, 789–799, 1993.

Garfinkel, C. I., and Hartmann, D. L.: Different ENSO teleconnections and their effects on the stratospheric polar vortex, J. Geophys. Res., 113, D18114, doi:10.1029/2008JD009920, 2008.

Garfinkel, C. I., Hartmann, D. L., and Sassi, F.: Tropospheric precursors of anomalous Northern Hemisphere stratospheric polar vortices, J. Climate, 23, doi:10.1175/2010JCLI3010.1, 2010.

Gelman, M. E., Miller, A. J., Johnson, K. W., and Nagatani, R. M.: Detection of long–term trends in global stratospheric temperature from NMC analyses derived from NOAA satellite data, Adv. Space Res., 6(10), 17–26, 1986.

Haigh, J. D., and Roscoe, H. K.: Solar influences on polar modes of variability, Meteologische Zeitschrift, 15, 371–378, 2006.

Holton, J. R., and Tan, H.–C.: The Influence of the equatorial quasi–biennial oscillation on the global circulation at 50 mb, J. Geophys. Res., 37, 2200–2208, 1980.

Hurwitz, M. M., Song, I.–S., Oman, L. D., Newman, P. A., Molod, A. M., Frith, S. M., and Nielsen, J. E.: Response of the Antarctic stratosphere to warm pool El Niño events in the GEOS CCM, Atm. Phys. Chem. Discuss., 11, 9743–9767, 2011.

Kalnay, E., Kanamitsu, M., Kistler, R., Collins, W., Deaven, D., Gandin, L., Iredell, M., Saha, S., White, G., Woollen, J., Zhu, Y., Chelliah, M., Ebisuzaki, W., Higgins, W., Janowiak, J., Mo, K. C., Ropelewski, C., Wang, J., Leetmaa, A., Reynolds, R., Jenne, R., Joseph, D.: The NCEP/NCAR 40–year reanalysis project, Bull. Amer. Meteor. Soc., 77, 437–471, 1996.

Kennedy, J., and Parker, D.: Global and regional climate in 2009, Weather, 65 (9), 244–250, 2010.

Kanamitsu, M., Ekisuzaki, W., Woollen, J., Yang, S.–K., Hnilo, J. J., Fiorino, M., and Potter, G. L.: NCEP–DOE AMIP–II reanalysis (R–2), Bull. Amer. Meteor. Soc., 83, 1631–1643, 2002.

Lu, H., Baldwin, M. P., Gray, L. J., and Jarvis, M. J.: Decadal–scale changes in the effect of the QBO on the northern stratospheric polar vortex, J. Geophys. Res., 113, D10114, doi:10.1029/2007JD009647, 2008.

Mantua, N. J., Hare, S. R., Zhang, Y., Wallace, J. M., and Francis, R. C.: A Pacific interdecadal climate oscillation with impacts on salmon production, Bull. Amer. Meteor. Soc., 78, 1069–1079, 1997.

Nagatani, R. M., Miller, A. J., Johnson, K. W., and Gelman, M. E.: An eight–year climatology of meteorological and SBUV ozone data, NOAA Tech. Rep. NWS 40, 125 pp., Natl. Weather Serv., Washington, D. C., 1988.

Nakamura, H., Lin, G., and Yamagata, T.: Decadal climate variability in the North Pacific during the recent decades, Bull. Amer. Meteorol. Soc., 78, 2215–2225, 1997.

Nash, E. R., Newman, P. A., Rosenfield, J. E., and Schoeberl, M. R.: An objective determination of the polar vortex using Ertel's potential vorticity, J. Geophys. Res., 101, D6, 9471–9478, 1996.

Randel, W. J., Shine, K. P., Austin, J., Barnett, J., Claud, C., Gillett, N. P., Keckhut, P., Langematz, U., Lin, R., Long, C., Mears, C., Miller, A., Nash, J., Seidel, D. J., Thompson, D. W. J., Wu, F., Yoden, S.: An update of observed stratospheric temperature trends, J. Geophys. Res., 114, D02107, doi:10.1029/2008JD010421, 2009.

Rayner, N. A., Parker, D. E., Horton, E. B., Folland, C. K., Alexander, L. V., Rowell, D. P., Kent, E. C., and Kaplan, A.: Global analyses of sea surface temperature, sea ice, and night marine air temperature since the late nineteenth century, J. Geophys. Res., 108, 4407, doi:10.1029/2002JD002670, 2003.

Rex, M., Salawitch, R. J., von der Gathen, P., Harris, N. R. P., Chipperfield, M. P., and Naujokat, B.: Arctic ozone loss and climate change, Geophys. Res. Lett., 31, L04116, doi:10.1029/2003GL018844, 2004.

Rex, M., Salawitch, R. J., Deckelmann, H., von der Gathen, P., Harris, N. R. P., Chipperfield, M. P., Naujokat, B., Reimer, E., Allaart, M., Andersen, S. B., Bevilacqua, R., Braathen, G. O., Claude, H., Davies, J., De Backer, H., Dier, H., Dorokhov, Fast, H., Gerding, M., Godin–Beekmann, S., Hoppel, K., Johnson, B., Kyro, E., Litynska, Z., Moore, D., Nakane, H., Parrondo, M. C., Risley, A. D., Skrivankova, P., Stubi, R., Viatte, P., Yushkov, V., Zerefos, C.: Arctic winter 2005: implications for stratospheric ozone loss and climate change, Geophys. Res. Lett., 33, L23808, doi:10.1029/2006GL026731, 2006.

Shine, K. P., Bourqui, M. S., Forster, P. M. D., Hare, S. H. E., Langematz, U., Braesicke, P., Grewe, V., Ponater, M., Schnadt, C., Smiths, C. A., Haigh, J. D., Austin, J., Butchart, N., Shindell, D. T., Randel, W. J., Nagashima, T., Portmann, R. W., Solomon, S., Seidel, D. J., Lanzante, J., Klein, S., Ramaswamy, V., Schwarzkopf, M. D.: A comparison of model–simulated trends in stratospheric temperatures, Q. J. Royal. Meteorol. Soc., 129, 590, 1565–1588, 2003.

SPARC CCMVal: SPARC Report on the Evaluation of Chemistry–Climate Models, V. Eyring, T. G. Shepherd, D. W. Waugh (Eds.), SPARC Report No. 5, WCRP–132, WMO/TD–No. 1526, http://www.atmosp.physics.utoronto.ca/SPARC, 2010.

Stolarski, R. S., Douglass, A. R., Newman, P. A., Pawson, S., and Schoeberl, M. R.: Relative contribution of greenhouse gases and ozone–depleting substances to temperature trends in the stratosphere: a chemistry–climate model study, J. Climate, 23, 26–42, 2010.

Stolarski, R. S., and Frith, S. M.: Search for evidence of trend slow–down in the long–term TOMS/SBUV total ozone data record: the importance of instrument drift uncertainty, Atmos. Chem. Phys., 6, 4057–4065, doi:10.5194/acp–6–4057–2006, 2006.

Trenberth, K. E.: The definition of El Niño, Bull. Amer. Met. Soc., 78, 2771–2777, 1997.

World Meteorological Organization (WMO): Scientific assessment of ozone depletion: 2010, Global Ozone Research and Monitoring Project, Rep. No. 52, 516 pp., Geneva, Switzerland, 2011.

Zhang, Y., Wallace, J. M., and Battisti, D. S.: ENSO–like interdecadal variability: 1900–93, J. Climate, 10, 1004–1020, 1997.

Figure Captions

Figure 1. Histograms of total ozone and dynamical conditions during the 1979–2011 period: (a) March total ozone averaged between 60–80°N [DU]; (b) March Arctic polar cap temperature at 50 hPa [K]; (c) Date of the Arctic vortex breakup at 450 K based on the NCEP–2 (black), NCEP–1 (light gray) and CPC (dark gray) reanalyses, binned into 10–day intervals; (d) January–February–March SST anomaly in the Niño 3.4 region [K]; (e) March zonal winds in the equatorial region at 50 hPa [m s^{-1}]; (f) January/February SST anomaly in the 40–50°N, 160–200°E region [K]. Red (blue) outlines indicate the location of 2011 (1997) conditions. Y–axis values indicate the mid–point of each histogram bin.

Figure 2. Meridional eddy heat flux at 40–80°N, 100 hPa [K m s^{-1}] in February as a function of Arctic polar cap temperature at 50 hPa [K] in March. Eddy heat flux and temperature values are denoted by year number (e.g., "11" denotes 2011).

Figure 3. March temperature differences [K] in the NCEP–2 reanalysis: (a) 2011 from the 1979–2011 climatological mean; (b) 1997 from the climatological mean; (c) composite of La Niña events from the climatological mean; (d) QBO–westerly as compared with QBO–easterly years. (e) March temperature differences for years when SSTs in the 40–50°N, 160–200°E region are more (less) than one standard deviation greater (less than) the climatological mean. In (c), (d) and (e) black Xs denote differences significant at the 95% confidence level. Zero difference contours are shown in white.

Figures

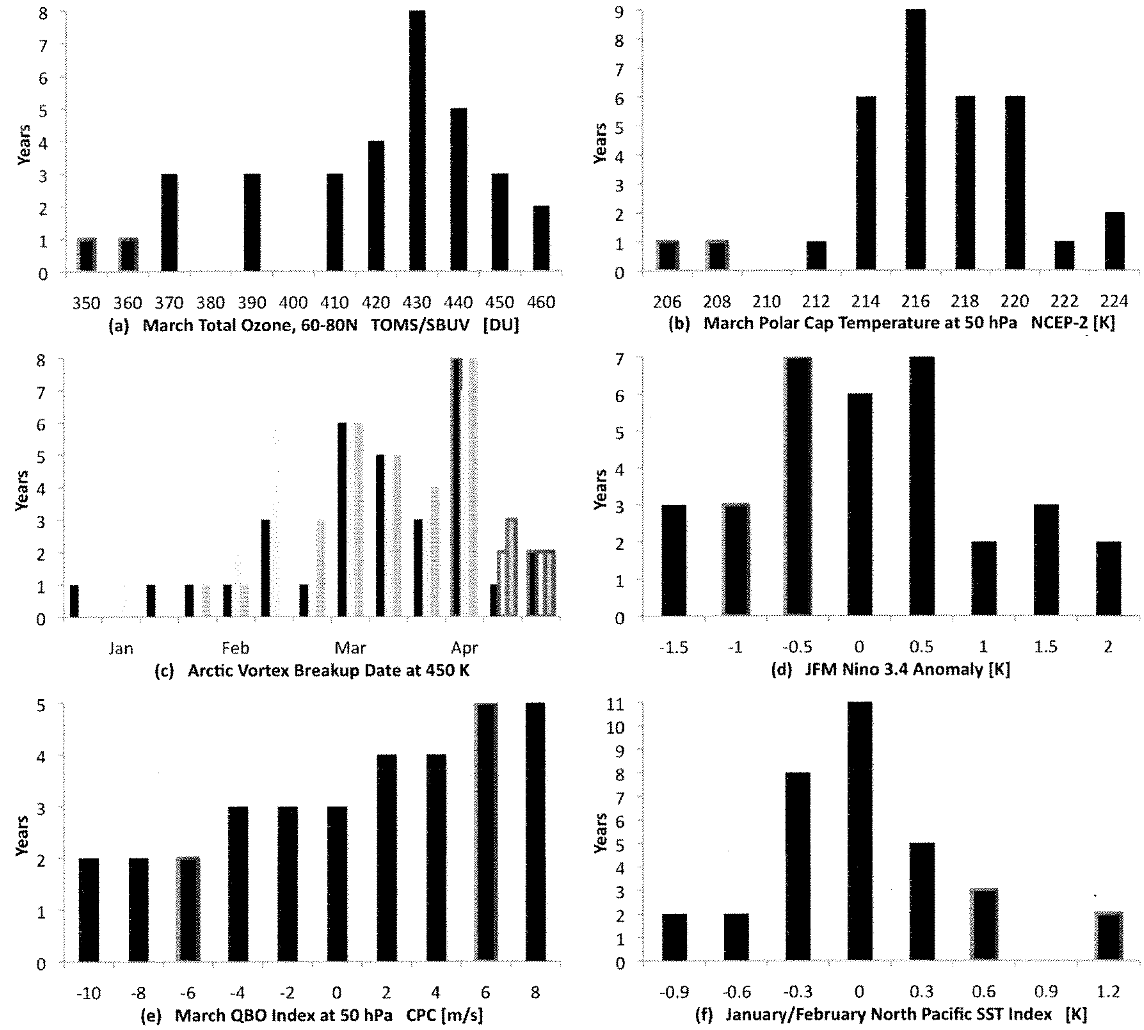

Figure 1

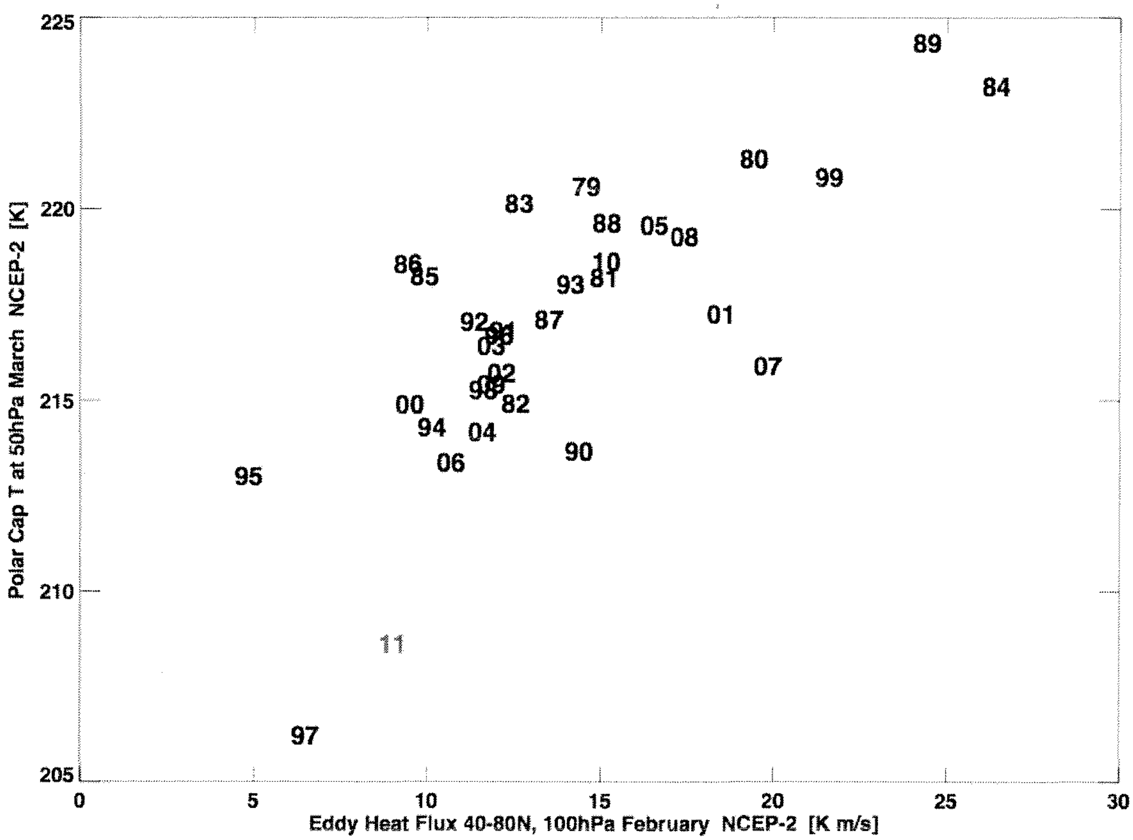
Polar Cap T at 50hPa March NCEP-2 [K]
Eddy Heat Flux 40-80N, 100hPa February NCEP-2 [K m/s]
225
220
215
210
205
0
5
10
15
20
25
30
89
84
80
99
79
83
88
05
08
10
86
85
93
81
01
92
87
03
07
02
82
00
94
04
90
06
95
11
97

Figure 2

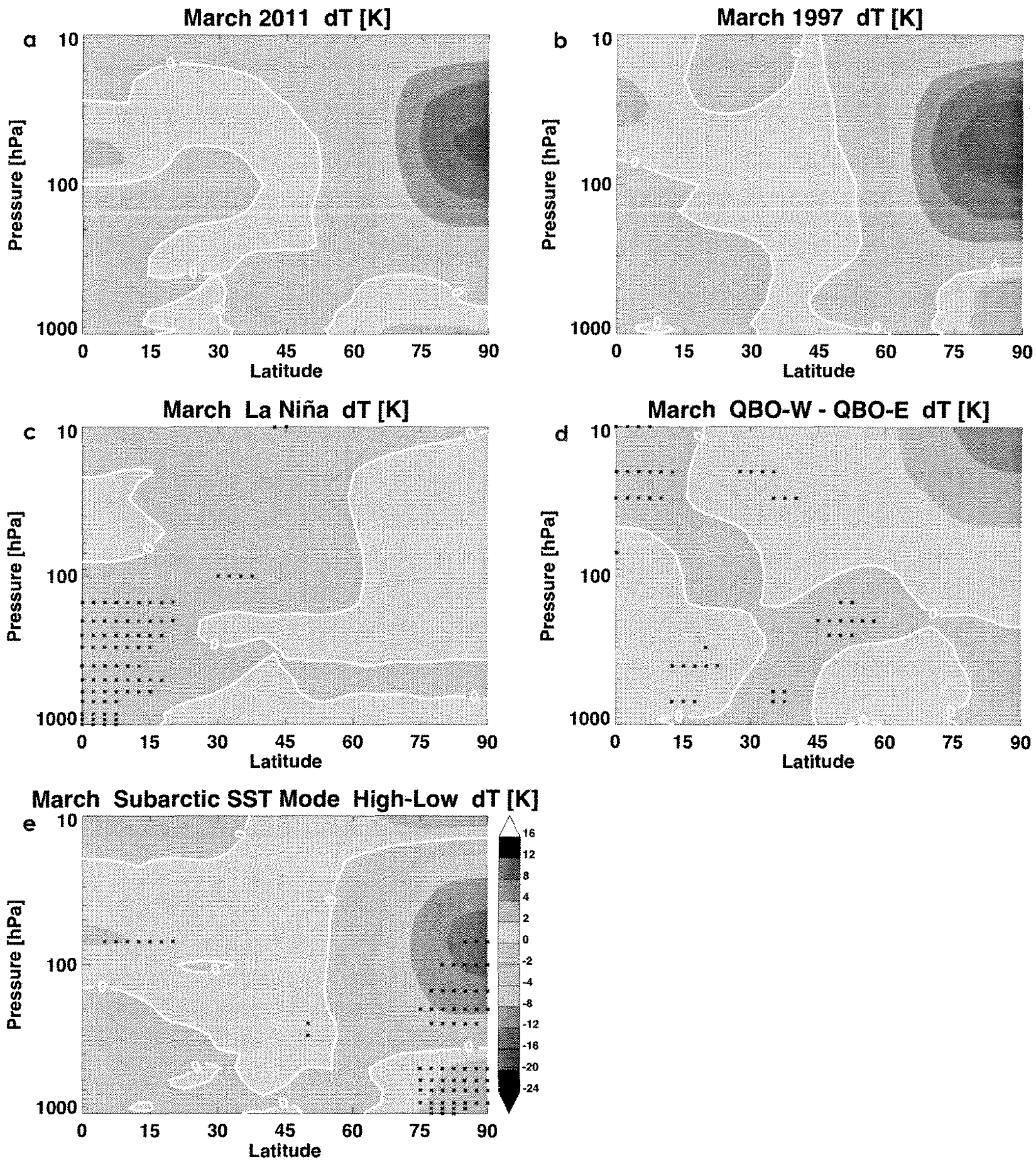
a
March 2011 dT [K]
b
March 1997 dT [K]
c
March La Niña dT [K]
d
March QBO-W - QBO-E dT [K]
e
March Subarctic SST Mode High-Low dT [K]
Pressure [hPa]
10
100
1000
Latitude
0
15
30
45
60
75
90
16
12
8
4
2
0
-2
-4
-8
-12
-16
-20
-24

Figure 3